Volume 12
Number 43
21 November 2021
Pages 6191-6364

Polymer Chemistry

rsc.li/polymers

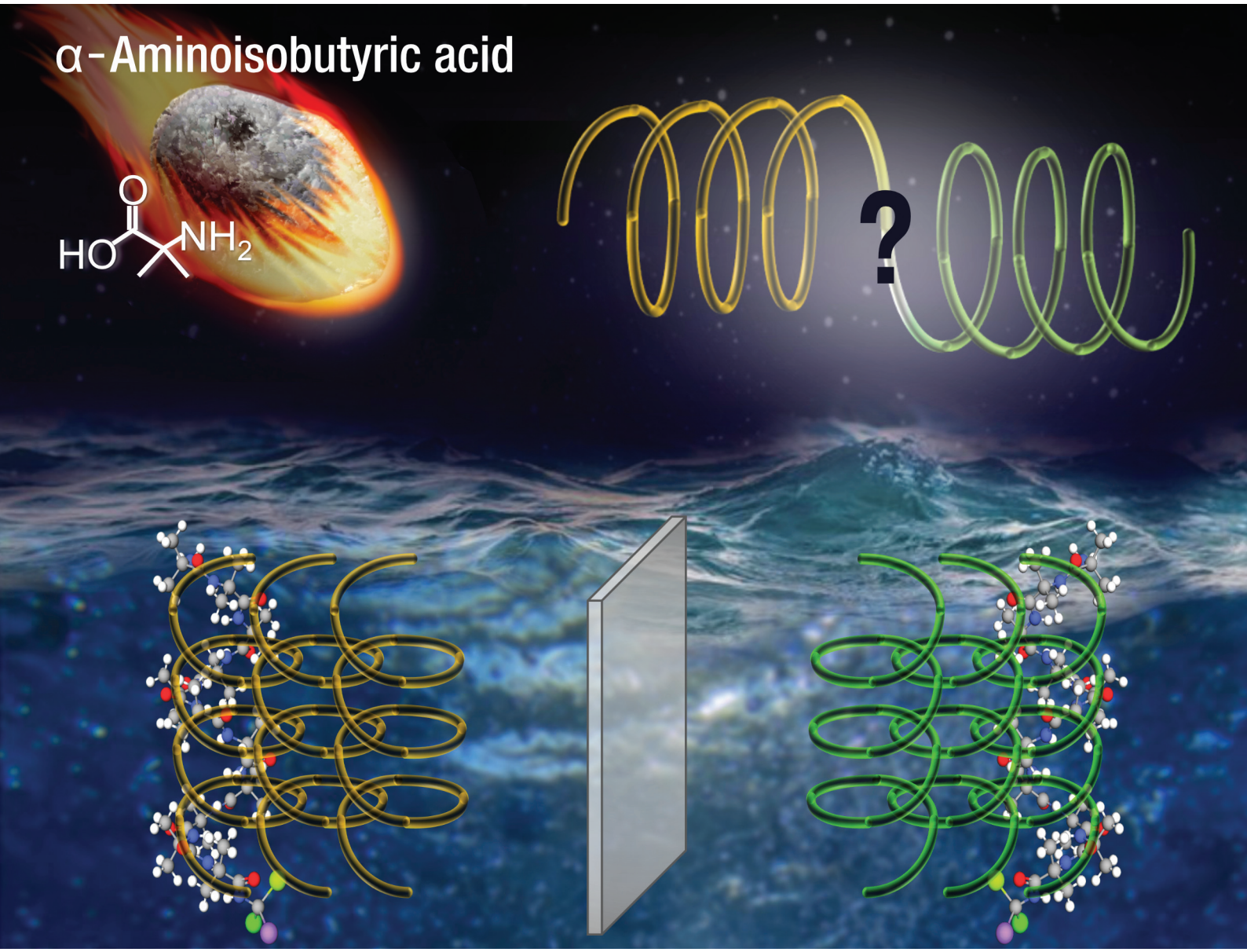

ISSN 1759-9962

ROYAL SOCIETY OF CHEMISTRY

PAPER
Wolfgang H. Binder *et al.*
Chiral amines as initiators for ROP and their chiral induction on poly(2-aminoisobutyric acid) chains

Polymer Chemistry

ROYAL SOCIETY OF CHEMISTRY

PAPER

View Article Online
View Journal | View Issue

Cite this: *Polym. Chem.*, 2021, **12**, 6252

Chiral amines as initiators for ROP and their chiral induction on poly(2-aminoisobutyric acid) chains†

Matthias Rohmer,‡[a] Özgün Ucak,‡[a] Rahul Fredrick[b] and Wolfgang H. Binder *[a]

2-Aminoisobutyric acid (Aib) is a prominent achiral amino acid known for its helical building properties, generating left- and right-handed helices without any preference. We here report an investigation on several short chain poly(Aib)s synthesized by ring opening polymerization (ROP) of Aib-*N*-carboxy-anhydrides (Aib-NCA) with structurally different chiral amines acting as both, initiator and chiral induction agent. To achieve the desired structures with a degree of polymerization of 10 up to 20 repeating units, different synthetic techniques such as solution and interfacial polymerization have been used leading to improved purity and precise end group control of the resulting polymers as confirmed by MALDI-ToF-MS and ^{1}H-NMR spectroscopy. By adding a chiral center at the C-terminus of the polymer chain we can control the direction of the screw sense, since the polymers are adopting the chirality of the initiator following the sergeant-and-soldier principle. Circular-Dichroism (CD) spectroscopy measurements revealed an exceptionally good chiral induction by the investigated initiators. Furthermore, variation of the solvent from hexafluoroisopropanol (HFIP) to water resulted in a significant change of CD signals, featuring a surprising aggregation of the poly(amino acids) into globular aggregates in water in the range of 50 to 200 nm, which accounts for changes in chiral induction.

Received 29th July 2021,
Accepted 27th September 2021

DOI: 10.1039/d1py01021b

rsc.li/polymers

Introduction

Biological systems can intrinsically self-assemble into helically ordered structures by virtue of hydrogen bonding,[1] hydrophobic interactions,[2] and van der Waals forces[3] to execute the essential functions for continuation of vitality.[4] The helix is a largely encountered self-assembled motif in nature, structurally forming α-helices and 3_{10} helices in proteins,[5,6] or super helices in DNA.[7] Chirality, a unique characteristic of living systems, potentially emerging as either left- or right-handed helical conformations from molecular to macroscopic dimensions, has an outstanding impact to self assemble into higher-order structures.[8,9] As biological systems possess predominant one-handed helicity as a chiral structure, one key step in order to mimic nature is well-defined control over the helical screw-sense. So far various synthetic helical chiral systems have been created by means of sergeant-and-soldier[10] and domino principles, such as poly(acetylene)s,[11] poly(phenylacetylene)s,[12] poly(phenyl isocyanide)s,[13] polyisocyanates,[14] polymethacrylates,[15] poly(carbodiimide)s[16] and polyisocyanides.[17]

α-Aminoisobutyric acid (Aib), an achiral non-proteinogenic amino acid, is already known as a helix promoter on account of its steric constraints that are induced by its geminal dimethyl group,[18] and has been already intensively investigated to induce helicity in peptides.[8,19–22] In addition, supramolecular chiral assemblies can result not only from chiral monomers, but also directly from achiral monomers by virtue of chiral initiators[23] like chiral amino acids,[24,25] catalyst systems,[12,13,16] solvents[26–28] or additives[29] by helix-sense-selective polymerization.[30] As achiral molecules exhibit neither a left- nor right-handed helicity preference due to a low inversion energy barrier, appropiate strategies for induction and transfer of chirality are fundamental to develop chiral helical polymer materials. Aib octamers are building 3_{10} helices with such a low inversion energy barrier that the helical conformation interconverts rapidly in solution.[31,32] It is already described in literature that by influence of a chiral amino acid at the N-[33] or C-terminus[24,25] of an Aib-chain either left- or right-handed helices can be induced.[34] The handedness of the Aib-chain is then defined by the conformation of the β-turn at the end of the 3_{10} helix,[35] which in turn can be controlled most effectively by hydrogen bonds.[35] This enables screw sense control of the Aib-chains[36] not only *via* chiral groups at the Aib-chain end, but also by interactions with ligands,[35,37] the solvent[34,38] and *via* pH effects.[36] Chiral information then proceeds through the Aib-chain by induction of a certain screw sense[39] up to a chain length of 20 monomers.[38] This interesting

[a]*Martin-Luther University Halle Wittenberg, Chair of Macromolecular Chemistry, D-06120 Halle, Germany. E-mail: wolfgang.binder@chemie.uni-halle.de*
[b]*Martin-Luther University Halle Wittenberg, Chair of Polymer Reaction Engineering, D-06099 Halle, Germany*

†Electronic supplementary information (ESI) available. See DOI: 10.1039/d1py01021b

‡Shared first authorship.

feature of Aib polymers could be used to mimic signaltransmission in biological systems as part of membran proteins.[37,40,41]

Ring opening polymerizations (ROP) has been successfully applied for the preparation of helical structures from chiral *N*-carboxyanhydride (NCA) monomers. Recently, we have reported the successfull helix-sense-selective polymerization of achiral Aib–NCA monomers by using chiral amino acid methyl ester initiatiors.[42] However the influence of different chiral initiators in a broder context, for example those with largely distant chiral entities or those sterically crowded and without aditional hydrogen bonding groups has not been reported yet.

In this work, we report a systematic investigation on induction of molecular chirality into supramolecular assemblies by interfacial and solution state ROP of Aib-NCA with different structured (*R*)- and (*S*)-enantiomeric chiral amine initiators. Herein we demonstrate how defined chirality of a molecule can be transferred to a supramolecular self assembly and how a single-handed helix screw sense preference can be amplified through the polypeptide chain. In addition, the ROP of NCA monomers enables us to prepare well defined synthetic polypeptides on a large scale without complicated time consuming procedures, focusing on both solution and interfacial polymerization strategies, thus presenting an alternative method to the solid phase synthesis *via* a peptide synthesiser.[24] Even though the polymerization in homogeneous medium is amost widely applied methodology, also polymerization in suspension phase has been reported.[43–47,48] Herein, we also address the influence of the solvent on the formation of the helices when differnt initiators are used, revealing a pronounced assembly of the helices in aqueous solvents.

Experimental part

Materials

The chiral amines were purchased from Sigma-Aldrich and were used without further purification. Hexafluoroisoropanol (HFIP) was purchased from Carbolution Chemicals. Triphosgene and 2-aminoisobutyric acid were purchased from ABCR. All solvents were dried prior to use. DMF, dioxane and acetonitrile were passed through a solvent purifying system. Heptane and hexane were dried over sodium and benzophenone and were freshly distilled under nitrogen atmosphere prior to use. Ethyl acetate was dried over P_2O_5. Deuterated chloroform ($CDCl_3$-d) and deuterated DMSO (DMSO-d_6) were purchased from Chemotrade; deuterated 1,1,1,3,3,3-hexafluoro-2-propanol (HFIP-d_2) from Armar.

Methods

Nuclear magnetic resonance (NMR) spectra were recorded on a Varian Gemini 400 NMR spectrometer (400 or 500 MHz) at 27 °C while using deuterated solvents as lock and the residual solvent signal as internal reference. All chemical shifts are given in ppm and all coupling constants in Hz. For interpretation of NMR-data MestReNova software (Version 11.0.0.17609) was used.

CD Spectroscopy was performed on a JASCO J-1500 with a PTC-510 cell holder. Samples were measured in a 1 mm cuvette (c = 0.2 mg mL^{-1}) or 10 mm cuvette (c = 0.02 mg mL^{-1}) at a wavelength range from 185 nm to 260 nm with a scanning speed of 100 nm min^{-1} with 20 accumulations. Baseline subtraction of the corresponding solvent has been conducted to obtain the corrected spectra. The samples were dissolved either in HFIP or in a water–HFIP mixture (water : HFIP ratio 95 to 5 v/v). For the dissolution of polymers in water–HFIP mixture the polymer was firstly dissolved in HFIP as a stock solution and was then added to water in a 95 to 5 ratio. Measurements in pure water were not possible due to the poor solubility of the prepared polymers in water. Data analysis was performed by Spectra Analysis and the secondary structure content was estimated by CD multivariate SSE program of JASCO Spectra Manager™ and the online tool BestSel.

Matrix-assisted laser desorption/ionization time-of-flight mass spectrometry (MALDI-ToF MS) was performed on a Bruker Autoflex III system (Bruker Daltonics) using a nitrogen laser operating at a wavelength of λ = 337 nm in reflection mode. The used matrix : analyte : salt ratio was 100 : 10 : 1 and 1 μL of the mixture was spotted on the MALDI target. The polymer samples were either dissolved or suspended in HFIP or DMF with a concentration of 10 mg mL^{-1} and dithranol was used as matrix adjusting a concentration of 20 mg mL^{-1} in THF, while KTFA was used as salt with a concentration of 5 mg mL^{-1} in THF. Data evaluation was carried out *via* flexAnalysis software (3.4) and simulation of the isotopic pattern was performed by Data Analysis software (version 4.0).

Transmission Electron microscopy (TEM) was performed on a electron microscope EM 900 from Zeiss with an acceleration voltage of 80 kV. A 5 μL diluted sample ($C_{polymer}$ = 0.2 or 0.02 mg mL^{-1} in water/HFIP mixture 95 to 5 v/v) was dropped on Formvar/Carbon film coated Cu grids and incubated for three minutes. The grids were blotted and gently washed with double distilled water minimum three times for one minute. Then, the grids were incubated with negative stain uranyl acetate (1% w/v) for one minute and blotted until completely dry. The dried grids were further dried 24 hours on filter paper before performing TEM.

Dynamic light scattering (DLS) measurements were performed on a DLS 802 by Viscotek in a 1.5 mL quartz cuvette with a polymer concentration of 0.2 mg mL^{-1} in HFIP and water/HFIP mixture.

Synthetic procedure

Synthesis of Aib-NCA monomer

Aib-NCA was synthesized according to our previously published procedure.[42]

Synthesis of Aib polypeptides *via* ROP in solution state

In a typical procedure for a solution state ROP of Aib-NCA, the Aib-NCA (M_n = 129.11 Da, $[NCA_0]$ = 1 mol L^{-1}, 2 mol L^{-1} or

0.77 mol L^{-1}) was dissolved in 1 mL solvent of either dimethylformamide, dioxane or acetonitrile in a Schlenk tube. To this solution, initiator was added with an Eppendorf pipette directly under a counter flow of nitrogen. The solution was stirred under an atmosphere of dry nitrogen at RT or heated to 80 °C or 40 °C in an oil bath. The reaction mixture was stirred overnight at 80 °C (or 2 days at 40 °C or 4 days at RT) and completeness of reaction was checked by FTIR spectroscopy. The purification of the polymer was performed by dialysis of the resulting polymer suspension in acetone for 2 days. The polymers were dried under vacuum.

Synthesis of Aib polypeptides *via* ROP *via* interfacial/suspension

Interfacial ROP of Aib-NCA was conducted according to previously published procedures with minor changes.[43–47] Aib-NCA was added to the Schlenk flask as a finely ground powder and was suspended in dry heptane or hexane ($c_{\text{Aib-NCA}}$ = 1 mmol mL^{-1}). Following addition of the liquid initiator by an Eppendorf pipette the suspension was heated to 40 °C and stirred at this temperature for two days under an atmosphere of dry nitrogen. The mixture was concentrated to dryness and washed with acetonitrile for several times to remove unreacted monomer. The resulting polymer was dried under vacuum.

Results and discussion

Synthesis of poly(Aib)s *via* ROP with chiral amines as initiators and characterization by MALDI-ToF MS

First, the Aib-NCA monomer (Scheme 1b) was synthesized from Aib (Scheme 1a) according to our previously published procedure.[42] The resulting Aib-NCA was obtained in 60% yield with high purity after several recrystallization steps. The structure of Aib-NCA monomer was confirmed by ^{1}H- and ^{13}C-NMR (see ESI, Fig. S1†).

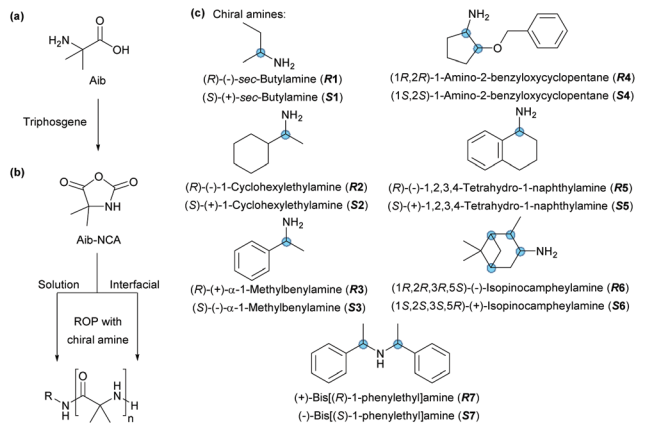

Scheme 1 (a) Aib NCA synthesis by Leuchs' method. (b) Ring opening polymerization of Aib NCA *via* chiral amines in either solution or interfacial (suspension or solid) phase. (c) Enantiomeric chiral amine initiators. Chiral centers are marked as a blue dot.

Polypeptides from Aib-NCA were either prepared *via* interfacial ROP in nonpolar solvents such as heptane or hexane in which both, the monomer and the resulting polypeptide are not soluble,[43–47] or *via* conventional solution ROP in DMF, ACN or 1,4 dioxane. To investigate the effect of the structure and location of a chiral centre on transfer and amplification of molecular chirality according to the sergeants-and-soldiers principle, enantiomeric primary and secondary chiral amine pairs which additionally differ in steric crowding, the number of chiral centres and the chiral centre distance to the amine functional group were incorporated into the polypeptides. The used *R*/*S* enantiomerically pure initiators for ROP (***R*1–*R*7** and ***S*1–*S*7**) are shown in Scheme 1c.

The Aib-NCA monomer underwent ROP either in nonpolar solvents like heptane/hexane or in polar solvents such as DMF/1,4-dioxane/ACN. Effects of temperature, monomer concentration, phase state and solvent polarity on the degree of polymerization (n), the molecular weight (M_n) and eventual side reactions were examined with primary and secondary amine initiation systems (see Table 1).

First, the effect of temperature (80 °C, 40 °C, RT) in the same solvent (DMF), as well as the effect of monomer concentration (1 or 2 mol L^{-1}) while keeping the temperature and the solvent constant (40 °C, DMF) on ROP initiated by ***R*1** were investigated. The monomer to initiator ratio (M/I) was kept constant to 15. Besides, the influence of the phase state of the polymerization medium (suspension state in hexane, heptane; solution state in DMF, dioxane, ACN) were also investigated for all initiators (***R*1–7** and ***S*1–7**). Steric hindrance, structure and primary/secondary amine characteristics were determined by a variety of enantiomeric pair of initiators as shown in Scheme 1.

The conclusive effects of a variety of factors on ROP are presented in Table 1. All obtained polymers were analysed by MALDI-ToF MS to identify the chemical composition, chain length and molecular weight. SEC could not be applied to determine molecular weight and dispersity index due to the low solubility of the obtained polypeptides in all possible solvents for GPC, even in DMF.

In order to understand the effects of temperature[49,50] and monomer concentration on ROP of Aib-NCA, DMF was used as the solvent. The poly(Aib)s ***R*1–1**, ***R*1–4** and ***R*1–5** were obtained at 80 °C, 40 °C and RT respectively. To investigate effects of solvent polarity on polymerization, DMF was changed to the more polar solvent ACN while keeping the rest of the conditions unchanged (T = 40 °C & C_{Monomer} = 2 mol L^{-1}, see polymer ***R*1–6**). The full MALDI-ToF-MS spectrums of the polymers ***R*1–1**, ***R*1–4**, ***R*1–5** and ***R*1–6** can be seen in Fig. 1. MALDI-ToF MS analyses revealed that at lower temperatures (at 80 °C → 40 °C → RT, for ***R*1–1**, ***R*1–4** and ***R*1–5** respectively), polymers with lower molecular weights are obtained ($M_{n,RT}$ = 924 Da, (m/z M_n + K^+ = 962) for ***R*1–5**, Fig. 1), ($M_{n,40\ °C}$ = 1008 Da, (m/z M_n + K^+ = 1047) for ***R*1–4**, Fig. 1), ($M_{n,80\ °C}$ = 1094 Da, (m/z M_n + K^+ = 1132) for ***R*1–1**, Fig. 1). Side reactions in the polymerizations where DMF is used as the solvent were detected by MALDI-ToF-MS analysis. It is proved that high

Table 1 ROP of Aib-NCA initiated by various chiral amine initiators **1–7** under different reaction conditions

Entry	Initiator	Polymerization method[a]	Solvent	M/I	T (°C)	$C_{Monomer}$ (M)	Sample code	Yield (%)	MALDI-TOF-MS M_n[b] (Da) & Min-Max n[c]
1	*R*1	Solution	DMF	15	80	2	*R*1–1	34	1094 Da (n = 12) & 9–16
2	*R*1				40		*R*1–2	30	1008 Da (n = 11) & 9–22
3	*S*1				80		*S*1–3	33	1009 Da (n = 11) & 9–17
4	*R*1				40	1	*R*1–4	15	1008 Da (n = 11) & 9–17
5	*R*1				RT	2	*R*1–5	19	923 Da (n = 10) & 8–18
6	*R*1		ACN	15	40	2	***R*1–6**	23	1008 Da (n = 11) & 9–25
7	*S*1			40			***S*1–7**	38	1093 Da (n = 12) & 10–16
8	*R*1	Interfacial	Hexane	15	40	1	*R*1–8	6	923 Da (n = 10) & 8–17
9	*R*1		Heptane	40	40	1	*R*1–9	31	1094 Da (n = 12) & 7–22
10	*S*1						*S*1–10	15	1162 Da (n = 13) & 9–17
11	*R*2	Solution	DMF	15	80	2	*R*2–11	31	1233 Da (n = 13) & 11–16
12	*R*2					0.77	*R*2–12	34	1318 Da (n = 14) & 11–17
13	*S*2					2	***S*2–13**	62	1318 Da (n = 14) & 10–19
14	*R*2		Dioxane	40	40	2	***R*2–14**	35	1318 Da (n = 14) & 12–26
15	*R*2	Interfacial	Heptane	40	40	1	*R*2–15	54	1233 Da (n = 13) & 10–22
16	*S*3	Solution	DMF	15	80	2	***S*3–16**	77	1142 Da (n = 12) & 9–15
17	*R*3		Dioxane	40	40		***R*3–17**	52	1312 Da (n = 14) & 11–24
18	*R*3	Interfacial	Heptane	40	40	1	*R*3–18	59	1142 Da (n = 12) & 9–25
19	*S*4						*S*4–19	36	1337 Da (n = 14) & 11–17
20	*R*4						*R*4–20	31	1297 Da (n = 14) & 9–24
21	*S*4	Solution	Dioxane	40	40	2	***S*4–21**	64	1382 Da (n = 14) & 10–19
22	*R*4						***R*4–22**	53	1552 Da (n = 16) & 11–23
23	*R*5						***R*5–23**	51	1253 Da (n = 13) & 11–27
24	*S*5		DMF	15	80	2	***S*5–24**	72	1338 Da (n = 14) & 12–17
25	*R*5	Interfacial	Heptane	40	40	1	*R*5–25	48	1253 Da (n = 13) & 9–24
26	*R*6						*R*6–26	18	1428 Da (n = 15) & 11–25
27	*S*6	Solution	DMF	15	80	2	***S*6–27**	48	1344 Da (n = 14) & 11–21
28	*R*6		Dioxane	40	40		***R*6–28**	55	1344 Da (n = 14) & 12–21
29	*S*7		DMF	15	80		*S*7–29	33	1246 Da (n = 12) & 8–19
30	*R*7		ACN	20	40	0.77	*R*7–30	n.q[d]	—
31	*R*7	Interfacial	Heptane	20	40	0.77	*R*7–31	42	1246 Da (n = 12) & 8–18

[a] Solution polymerization was conducted in homogeneous medium whereas interfacial polymerization was conducted in the suspended phase. [b] Determined *via* the chain length (n) of the highest intensity in MALDI-TOF. [c] Chain length distribution. [d] Yield is not quantitative. MALDI-TOF-MS analysis could not be accomplished.

temperature triggers formation of backbiting side products during polymerization in DMF. In the MALDI-ToF MS spectra of ***R*1–1** (Fig. 1), m/z = 1132 represents the desired poly(Aib) chain bearing an amine end group and *sec*-butylamine at the C-terminus (see structure **II-I** in Scheme 2). However, end group analysis of the ***R*1–1** by MALDI-ToF MS (see Fig. 1) also indicates that there is an uncontrolled formation of the poly (Aib) with aldehyde end groups (see structure **II-II** in Scheme 2), in which the peaks at m/z = 1145 and m/z = 1161 correspond to the Na^+-/K^+-ions of the aldehyde terminated poly(Aib)s, resulting from a side reaction with DMF. Changing the polymerization medium to the more polar ACN has a high impact on obtaining pure polymers possessing controlled end groups (see ***R*1–6** in Fig. 1). The investigations show that by using lower temperatures and changing the solvent we were able to reduce side reactions. Moreover, basicity and steric hindrance of the amines were investigated by using different chiral amines (see Scheme 1c) as initiators for the ROP. MALDI-ToF MS revealed that under the same reaction-conditions, the results vary between different sterically hindered amines. The secondary amine **7** is less basic than primary amines, in turn leading to numerous side reactions during the ROP (see Fig. 2). MALDI-ToF MS revealed the occurrence of side reactions beside the Normal Amine Mechanism (NAM), because of the lower nucleophilicity of the chiral amine initiator **7** which leads to an abstraction of the hydrogen atom from *N*-carboxyanhydride (see Scheme 2). The nucleophilicity of the resulting activated NCA ring is sufficient to induce the polymerization by attacking the carbonyl group resulting in a polymerization according to the Activated Monomer Mechanism[51] (AMM structure **III** and **IV** in Scheme 2). In Fig. 2 the MALDI-ToF MS of ***S*7–29** and ***S*3–16** are displayed which are polymerized under the same conditions but the resulting polymers show different purity. ***S*3–16** is a pure polymer with the desired end group (structure **II-I**, Scheme 2) showing no side reactions in contrast to ***S*7–29**, which displays aquite a number of side peaks in the MALDI-ToF MS. The peaks at m/z = 1285 and m/z = 1269 are representing the desired polymer (structure **II-I**, Scheme 2) resulting from the NAM reaction, but the peaks at m/z = 1274 could be assigned to a polymer initiated by an activated NCA-ring (structure **IV-I**, Scheme 2) following the AMM. Furthermore, a side product represented by peaks at m/z = 1231 and m/z = 1247 could be assigned to structure **V-I** which is obtained after an AMM of Aib-NCA followed by an attack of water at the remaining NCA ring. These results of MALDI-ToF MS indicate a coexistence of

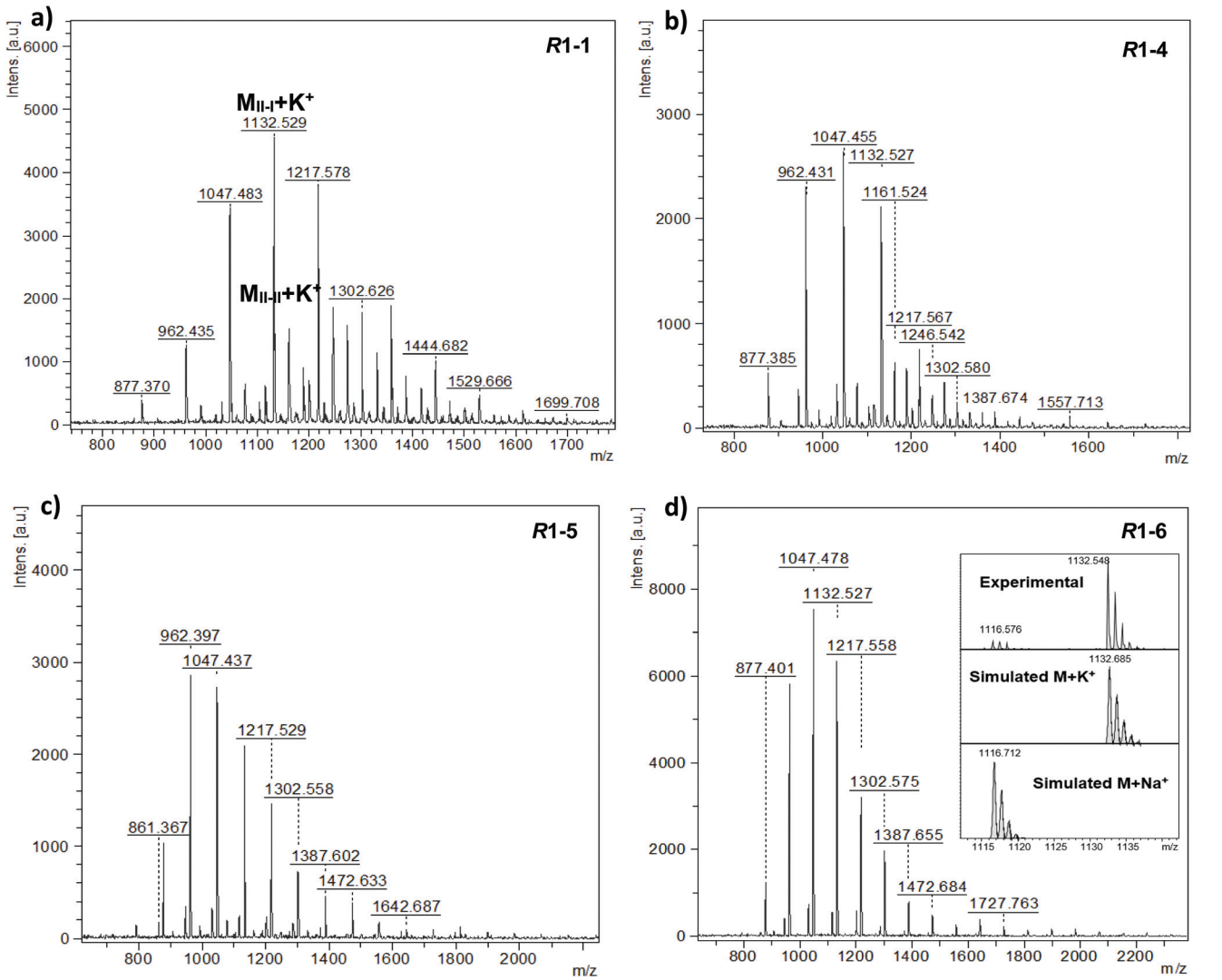

Fig. 1 (a) MALDI-ToF-MS spectra of polymer ***R*1–1**. (b) MALDI-TOF-MS spectra of polymer ***R*1–4**. (c) MALDI-ToF-MS spectra of polymer ***R*1–5**. (d) MALDI-ToF-MS spectra of polymer ***R*1–6** (see Table 1 for detailed polymerization conditions).

the NAM and AMM during the polymerization of Aib with the secondary amine **7**, thus leading to an uncontrolled polymerization. By changing the polymerization conditions similar to those of the primary amines, it was not possible to obtain a pure polymer, allowing the conclusion that the nucleophilicity of the secondary amine **7** is not sufficient for fast initiation. In case of solution polymerization, precipitation of the formed polymer could be observed. This leads to the limitation of the chain length and in some cases side reactions were taking place. To improve the end group control and purity of our polymers we probed interfacial ROP of Aib-NCA by suspending a fine crystalline powder of Aib-NCA in heptane by constant stirring. The Aib-NCA is not soluble in heptane but the initiator is. In this mode a polymerization takes place through an initiation at the interface of the solution and the Aib-NCA crystal surface. In Fig. 2 the MALDI-ToF MS of ***R*3–17** and ***R*3–18** are displayed showing particularly good end group control and the desired structures **II-I**. The chain length for interfacial polymerization ***R*1–17** is slightly higher when compared to solution polymerization, but the yield was often low. To sum up, in the ROP of Aib-NCA, the results indicate that decreasing the polymerization temperature from 80 to 40 °C reduces side reactions, being fully eliminated upon a solvent change to ACN or heptane. During solution phase polymerization of Aib, a precipitation of the resulting polymer was observed in DMF, dioxane and ACN, which probably limited the obtainable chain lengths. Interfacial polymerization leads to polymers with comparable good purity and slightly enhanced chain lengths, being a promising candidate for further investigations.

CD investigations of poly(Aib)s

Circular Dichroism (CD) spectroscopy is a fast and selective method to determine the secondary structure of poly(amino acids) and the conformation of the peptide in different sol-

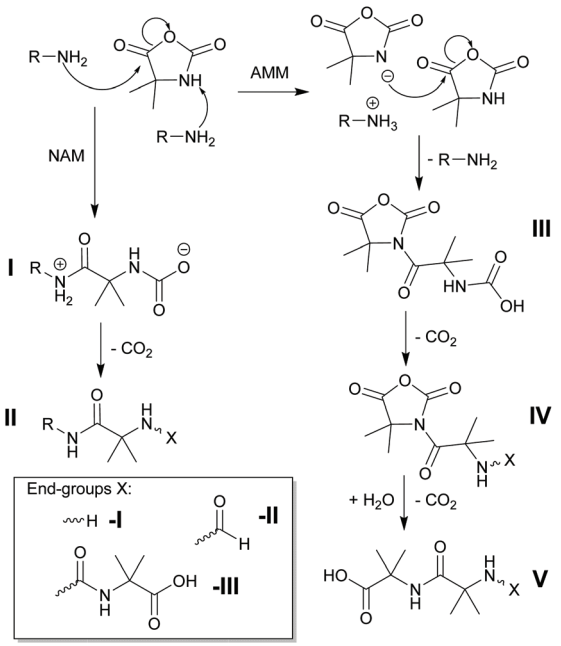

Scheme 2 Polymerization of Aib-NCA according to the Normal Amine Mechanism (NAM) and the Activated Monomer Mechanism (AMM) with possible end groups X from side reactions.

vents. CD spectroscopy measures the difference of the absorption of right- and left-handed light through the sample, which makes it the perfect tool to analyze the handedness of a screw sense, because secondary structures that adopt opposite handedness will absorb circular polarized light in opposite amounts, leading to a mirroring effect of the CD spectra. It is known that poly(Aib) adopts a 3_{10} helix without a preferred screw sense, resulting in no detectable CD signal.[22] By using a chiral group at the C-terminus of the chain we expected chiral induction into the polymer chain. If the chiral induction[52] following the sergeant-and-soldier principle is successful, then the detection of a CD signal should be possible and by changing the chirality of the group at the C-terminus the exact opposite CD spectra should be obtained,[33,42,53] a fact already reported in literature for chiral groups with hydrogen bonding groups, which can control the helicity of the Aib-chain. Herein the first β-turn is defined through hydrogen bonding with the chiral center then leading to a chiral induction. The expected CD spectra of a 3_{10} helix or an alpha helix are difficult to discriminate, as both are showing a strong maximum at 190 nm and only the intensity difference between the minima at λ = 208 and 222 nm can be used as a hint to discriminate them.[54–56] By detection and analysis of the CD signals we systematically investigated the chiral induction of structurally different chiral amines on the poly(Aib) chain in various solvents.

CD investigations are conducted in HFIP and a water/HFIP mixture in a ratio of 95 to 5 (v/v) to investigate the secondary structure formation of poly(Aib) and the chiral induction in different solvents. The resulting CD spectra are presented in Fig. 3, where polymers initiated by either (*S*)-, or (*R*)-initiators showed the respective inverted helices. The CD spectra in Fig. 3a, b, d and f are displaying very similar results, featuring a very good mirroring effect of the spectra depending on the chirality of the initiator. The intensity of the signals is quite low in HFIP but even though there probably is a chiral induction happening in this solvent. The small intensity indicates that the chiral induction is not strong in HFIP. In HFIP there is only a small maximum at 190 nm and a minimum around 220 nm detectable as can be seen best in the case of ***R*2–14** in Fig. 3b. In water/HFIP mixture the CD signals are more intense with a well-defined shape with two maxima at around 190 and 208 nm and two minima at 200 nm and between 220 and 230 nm. By changing the chirality of the chiral amine at the C-terminus of the polymer chain, the exact opposite CD spectra was obtained.

The CD spectra of the initiators with an aromatic group (**3** and **5** see Fig. 3c and e) are showing a different shape and a more pronounced intensity in HFIP. The polymers obtained by ROP with the chiral amine **3** are characterized by a similar CD spectrum in HFIP and water/HFIP mixture featuring a maximum at 192 nm with a shoulder around 205 nm, however in water/HFIP mixture there is an additional minimum at 225 nm. Polymers bearing the chiral amine **5** at the C-terminus of the chain show an intense CD signal in HFIP and in water/HFIP mixture. In HFIP a maximum at 186 nm and a minimum at 220 nm was detected as well as two shoulders at around 200 and 210 nm. The CD spectra of polymers with the initiator **5** in water/HFIP mixture are similar to the CD spectra of the remaining polymers with chiral amines (**1**, **2**, **4** and **6**) at the C-terminus. The CD spectra of the pure initiators were also measured to determine the influence of the initiator on the CD spectra of the polymer. As seen in Fig. 3c and e the initiators **3** and **5** are showing an absorption in the far UV region. The aromatic groups of the initiators have an influence on the CD spectra which probably alters the form of the CD spectra. By mixing the (*R*)- and (*S*)-amine initiated polymers the CD signals of these polymers were eliminated leading to an almost straight line with a CD intensity of zero.

Hydrogen bonds between the peptide groups play a crucial role in building and stabilization of secondary structures.[57,58] The alpha helix is stabilized by intramolecular hydrogen bonds every four peptide groups and the 3_{10} helix has hydrogen bonds every three peptide groups which leads to a preference of a 3_{10} helix above the alpha helix for short chains and to a stabilization of helical structures in polar solvents.[55,58,59] As seen in the CD spectra the polymers are not forming a regular alpha or 3_{10} helix with a typical two minima at λ = 208 and 222 nm. In HFIP only small intensity signals are obtained for most of the initiators (**1**, **2**, **4** and **6**). The CD signal looks like a very weak helical signal indicating that poly(Aib) forms a 3_{10} helix but due to a weak chiral induction the amounts of right- and left-handed helices are nearly the same. The initiators **3** and **5** show a different CD spectrum in HFIP (Fig. 3c and e) with intense signals indicating a good chiral induction. Polymer ***S*3–16** shows a maximum at 193 nm and a

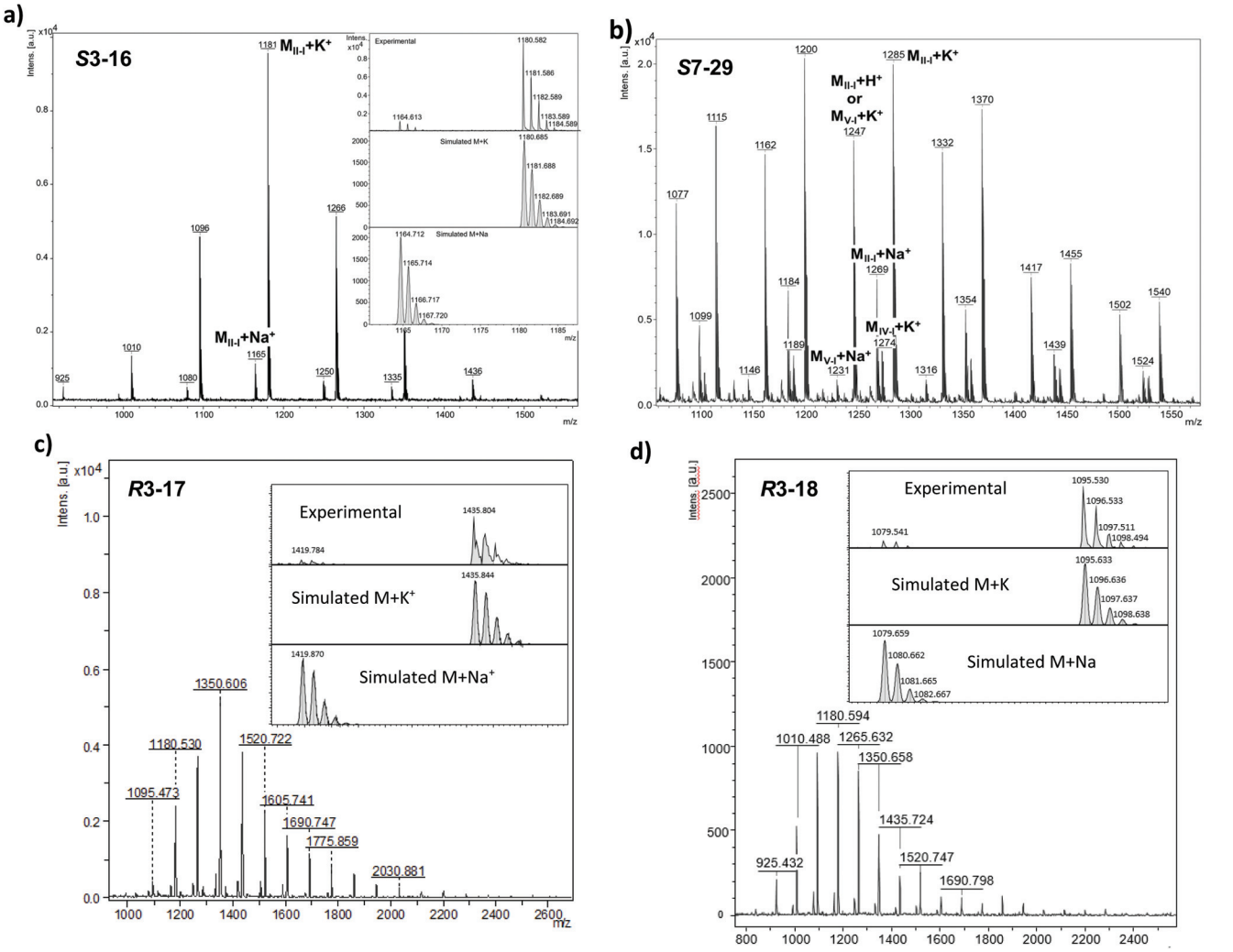

Fig. 2 (a) MALDI-ToF-MS spectra of polymer ***S*3–16**. (b) MALDI-ToF-MS spectra of polymer ***S*7–29**. (c) MALDI-ToF-MS spectra of polymer ***R*3–17** and (d) MALDI-ToF-MS spectra of polymer ***R*3–18** (see Table 1 for detailed polymerization conditions).

shoulder around 205 nm but no signal in the region of 220 to 230 nm. This is a very uncommon feature and it is the only polymer showing this form in the CD spectroscopy. The polymer obtained by ROP with the initiator **5** also shows a different CD spectrum in HFIP but a big influence of the aromatic group of the initiator has to be taken into account here. Nevertheless, there is a clear minimum at 220 nm and a shoulder like structure at 205 nm indicating a helical like structure. A huge difference in the CD spectra between measurements in HFIP and in water/HFIP mixture was observed for all polymers. In all cases we obtain strong CD signals indicating a good chiral induction and a similar form of the CD spectrum for the initiators **1**, **2** and **4** to **6** in water/HFIP mixture. The minima between 220 and 230 nm combined with the maxima at around 208 nm indicates a type III beta-turn[33] but the CD spectra below λ = 200 nm are more indicative of a distorted helix with a maximum at λ = 195 to 200 nm and a minimum between λ = 185 and 190 nm.[60,61] A suggestion would be that chiral induction leads to the formation of type III beta-turn which can stack into a distorted 3_{10} helix.[20] Because of the poor solubility in water there are only a few CD spectra of poly(Aib) in water in the literature, which are in good agreement with our results, indicating a successful chiral induction and 3_{10} helix formation in water.[24] For initiator **3** the difference between HFIP and water/HFIP mixture is not so pronounced but there is a very characteristic minimum at 225 nm that indicates a helical structure which was not present in HFIP.

The solvent thus seems to play an important role in the chirality transfer as well as in the different secondary structure formations according to the chirality of the initiator, which also might be due to an aggregation process[62] of the polymers taking place in the water/HFIP mixture as reported for other Aib-copolymers aggregating in aqueous media.[8] Aggregation was investigated by DLS and TEM (see Fig. 4), revealing the formation of globular aggregates in the range of 50 to 200 nm. Two potential mechanisms for the polymer aggregation can be assumed: first aggregation[63] might be induced through inter-

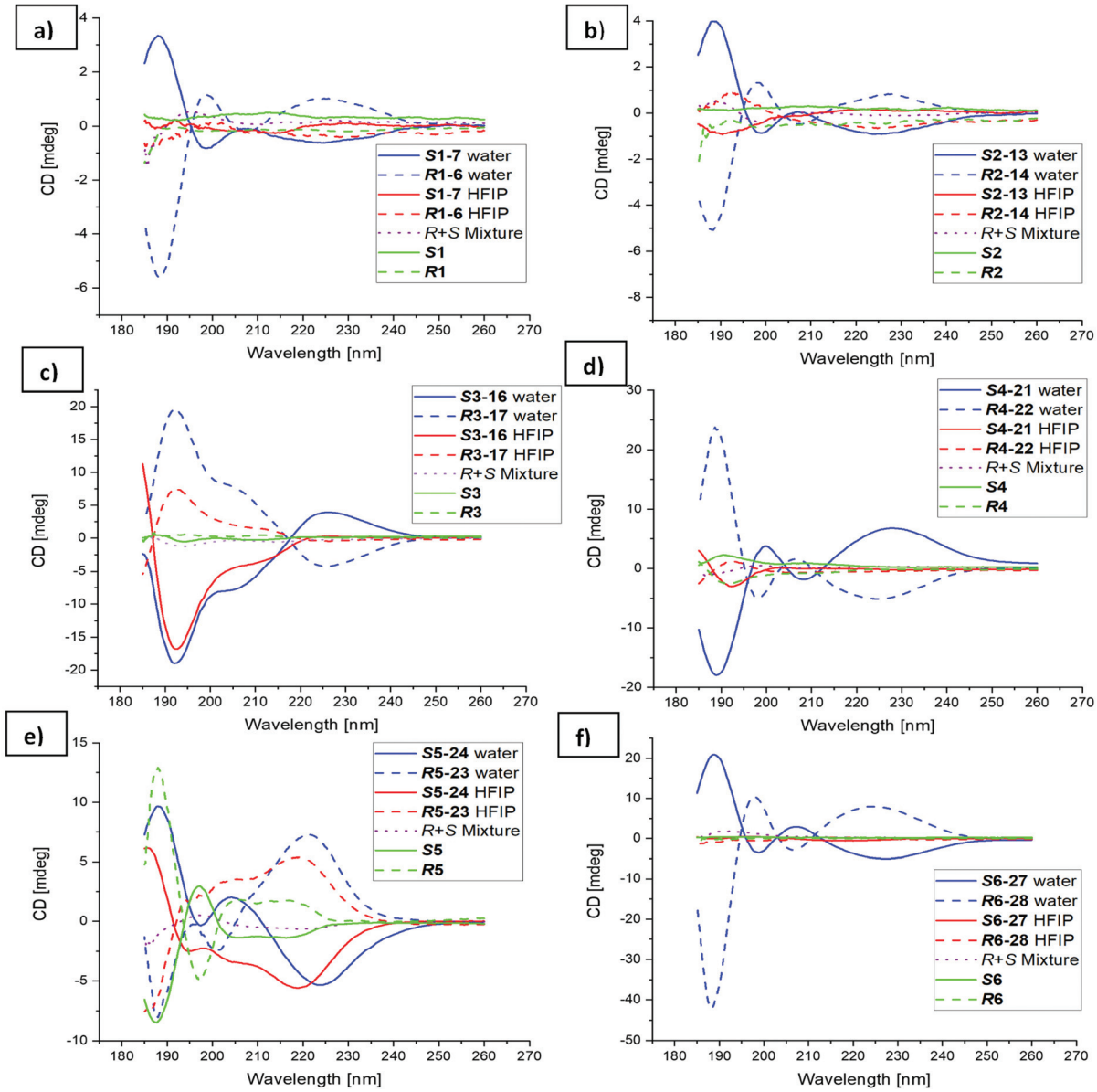

Fig. 3 CD Spectra (a–f) of poly(Aib) initiated with (*R*)- (dotted line) and (*S*)-amines (solid line) in water/HFIP mixture (blue) and HFIP (red) and the pure chiral amines in water/HFIP mixture (green).

molecular hydrogen bonding leading to stereo complex formation[64–66] and second it is known that HFIP aggregates in water due to its fluorinated groups. As HFIP starts to aggregate above 25% v/v HFIP,[67] we can exclude this effect here since we only use 5% v/v HFIP in our experiment. Thus we assume that the aggregation is originating from the intermolecular H-bonding. The aggregation seems to enhance the chiral induction by the amines at the C-terminus, reminiscent of poly(Aib) oligomers known to aggregate and build intermolecular hydrogen bonds between the helices in membrans.[40,68]

By using a secondary structure analysis program (CD Multivariate SSE from Jasco and online tool BestSel results shown in the ESI Tables S1 and S2†) we estimated the helicity and other secondary structure parts from the CD spectra. The results of the CD multivariate SSE and BestSel program show huge differences in the calculated secondary structure content. The calculated helical content is much higher by CD Multivariate SSE program then by the BestSel program, presumably because BestSel uses only the range between 200 and 250 nm to calculate the secondary structure content but the signals which might indicate a distorted helix are below 200 nm. Thus the BestSel program calculates a helical content of around 1% and a beta-turn content of 15% for all polymers. The (*R*)- and (*S*)-initiated polymers show very similar calculated secondary structure content by BestSel as expected by the very good mirroring effects in the CD spectra but the calculations with CD Multivariate SSE displays big differences between the (*R*)- and (*S*)-initiated polymers. As the CD Multivariate SSE

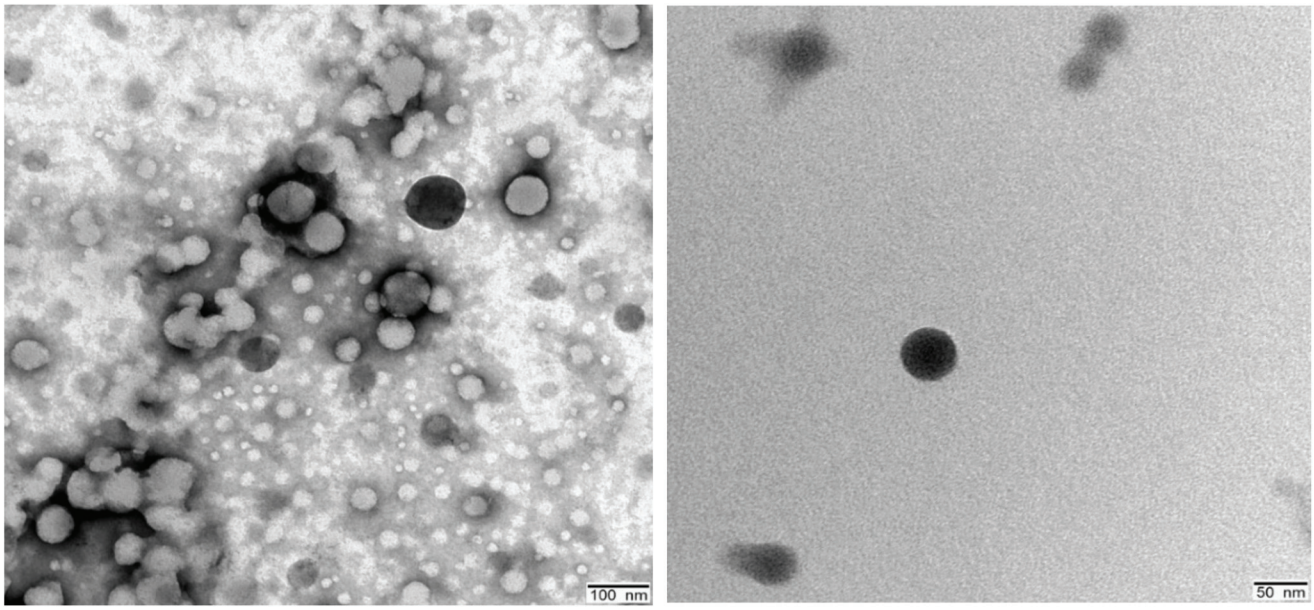

Fig. 4 TEM measurement of ***R*6–28** in water/HFIP mixture with a concentration of 0.2 mg mL^{-1} (left side) and 0.02 mg mL^{-1} (right side).

program is optimized for protein structures this might explain the variations of (*R*)- and (*S*)-initiated polymers. Both programs show a beta turn content of around 15 to 20% as suggested by the form of the CD spectra between 200 and 260 nm. Unfortunately, the calculated secondary structures are only an estimation based on a database, which does not include 3_{10} helices so the values are different from reality.

Conclusions

In this work we present the successful synthesis of pure poly(Aib)s bearing chiral amines at their C-terminus. We used different polymerization conditions in solution as well as interfacial polymerization to obtain well defined Aib-polymers with defined end groups as proven by MALDI-ToF MS and ^{1}H-NMR spectroscopy. Native poly(Aib) is achiral and has no preferred helical screw sense, but CD spectroscopy shows that our synthesised polymers have a preferred screw sense depending on the chirality of the affixed initiator group. The chirality of the headgroup at the C-terminus is defining the screw sense by chiral induction following the sergeant-and-soldier principle, which then proceeds through the chain. By changing the chirality of the initiator we are able to obtain the opposite handedness of the chain leading to a mirroring effect in the CD spectra. Furthermore, we found a strong solvent dependency of this chiral induction. In pure HFIP only two initiators (**3** and **5**) were showing a strong CD signal, leading to the hypothesis that chirality transfer is not sufficient in this solvent for the remaining initiators (**1**, **2**, **4** and **6**), while in water/HFIP mixture chiral induction is occurring in all cases leading to strong CD signals. The chirality induction can only take place *via* sterical reasons, as the used chiral amines do not have hydrogen bonding groups to determine the first β-turn. This influence on the Aib-chain is not pronounced in HFIP, but in water/HFIP mixture the induction of a specific screw sense is successful. This difference is due to an assembly process of the polymer chains in water leading to globular aggregates in the size of 50 to 200 nm. In these aggregates intermolecular hydrogen bonding is highly possible and water further stabilizes the helical structure. Thus our work demonstrates that a chiral induction can take place from an chiral amine without any hydrogen bonding groups at the C-terminus of an Aib-chain, depending strongly on the solvent and the aggregation processes. The exact secondary structure of these aggregates as well as the formation process *via* inter- and intramolecular interactions is presently a starting point for further investigations.

Author contributions

ÖU and MR both did experiments, conducted synthesis and CD-measurements, and interpreted results. ÖU und MR share first authorship equally. WHB, MR and ÖU wrote the paper; WHB designed research and financed research.

Conflicts of interest

There are no conflicts to declare.

Acknowledgements

We thank the DFG-Graduate College GRK 2670 (German research foundation – project ID 43649874, TP B2, RTG 2670);

the DFG-SFB TRR 102 Nr 189853844 and the Graduate School AGRIPOLY of the State Saxony Anhalt for financial support. We thank Dr Gerd Hause for providing the TEM pictures.

References

1 R. P. Sijbesma and E. W. Meijer, *Curr. Opin. Colloid Interface Sci.*, 1999, **4**, 24–32.
2 A. Sánchez-Iglesias, M. Grzelczak, T. Altantzis, B. Goris, J. Pérez-Juste, S. Bals, G. Van Tendeloo, S. H. Donaldson, B. F. Chmelka, J. N. Israelachvili and L. M. Liz-Marzán, *ACS Nano*, 2012, **6**, 11059–11065.
3 D. Lombardo, M. A. Kiselev, S. Magazù and P. Calandra, *Adv. Condens. Matter Phys.*, 2015, **2015**, 1–22.
4 N. Stephanopoulos, J. H. Ortony and S. I. Stupp, *Acta Mater.*, 2013, **61**, 912–930.
5 L. Pauling, R. B. Corey and H. R. Branson, *Proc. Natl. Acad. Sci. U. S. A.*, 1951, **37**, 205.
6 D. J. Barlow and J. M. Thornton, *J. Mol. Biol.*, 1988, **201**, 601–619.
7 J. D. Watson and F. H. C. Crick, *Nature*, 1953, **171**, 737–738.
8 I. Tarasenko, N. Zashikhina, I. Guryanov, M. Volokitina, B. Biondi, S. Fiorucci, F. Formaggio, T. Tennikova and E. Korzhikova-Vlakh, *RSC Adv.*, 2018, **8**, 34603–34613.
9 J. Solà, S. P. Fletcher, A. Castellanos and J. Clayden, *Angew. Chem., Int. Ed.*, 2010, **49**, 6836–6839.
10 M. M. Green, M. P. Reidy, R. D. Johnson, G. Darling, D. J. O'Leary and G. Willson, *J. Am. Chem. Soc.*, 1989, **111**, 6452–6454.
11 K. Nagai, T. Masuda, T. Nakagawa, B. D. Freeman and I. Pinnau, *Prog. Polym. Sci.*, 2001, **26**, 721–798.
12 T. Aoki, T. Kaneko, N. Maruyama, A. Sumi, M. Takahashi, T. Sato and M. Teraguchi, *J. Am. Chem. Soc.*, 2003, **125**, 6346–6347.
13 L. Xu, L. Yang, Z. Guo, N. Liu, Y.-Y. Zhu, Z. Li and Z.-Q. Wu, *Macromolecules*, 2019, **52**, 5698–5706.
14 Y. Okamoto, M. Matsuda, T. Nakano and E. Yashima, *Polym. J.*, 1993, **25**, 391–396.
15 Y. Okamoto and T. Nakano, *Chem. Rev.*, 2002, **94**, 349–372.
16 H.-Z. Tang, P. D. Boyle and B. M. Novak, *J. Am. Chem. Soc.*, 2005, **127**, 2136–2142.
17 Z.-Q. Wu, K. Nagai, M. Banno, K. Okoshi, K. Onitsuka and E. Yashima, *J. Am. Chem. Soc.*, 2009, **131**, 6708–6718.
18 C. Toniolo and E. Benedetti, *Macromolecules*, 1991, **24**, 4004–4009.
19 R. Banerjee, G. Basu, S. Roy and P. Chène, *J. Pept. Res.*, 2002, **60**, 88–94.
20 M. De Poli, M. De Zotti, J. Raftery, J. A. Aguilar, G. A. Morris and J. Clayden, *J. Org. Chem.*, 2013, **78**, 2248–2255.
21 G. Tsuji, T. Misawa, M. Doi and Y. Demizu, *ACS Omega*, 2018, **3**, 6395–6399.
22 A. Ueda, M. Oba, Y. Izumi, Y. Sueyoshi, M. Doi, Y. Demizu, M. Kurihara and M. Tanaka, *Tetrahedron*, 2016, **72**, 5864–5871.
23 H. Huang, J. Deng and Y. Shi, *Macromolecules*, 2016, **49**, 2948–2956.
24 F. Zieleniewski, D. N. Woolfson and J. Clayden, *Chem. Commun.*, 2020, **56**, 12049–12052.
25 B. A. F. Le Bailly and J. Clayden, *Chem. Commun.*, 2014, **50**, 7949–7952.
26 P. A. Korevaar, C. J. Newcomb, E. W. Meijer and S. I. Stupp, *J. Am. Chem. Soc.*, 2014, **136**, 8540–8543.
27 P. A. Korevaar, C. Schaefer, T. F. de Greef and E. W. Meijer, *J. Am. Chem. Soc.*, 2012, **134**, 13482–13491.
28 D. Lee, Y.-J. Jin, H. Kim, N. Suzuki, M. Fujiki, T. Sakaguchi, S. K. Kim, W.-E. Lee and G. Kwak, *Macromolecules*, 2012, **45**, 5379–5386.
29 H. Huang, Y. Yuan and J. Deng, *Macromolecules*, 2015, **48**, 3406–3413.
30 N. J. Van Zee, M. F. J. Mabesoone, B. Adelizzi, A. R. A. Palmans and E. W. Meijer, *J. Am. Chem. Soc.*, 2020, **142**, 20191–20200.
31 R.-P. Hummel, C. Toniolo and G. Jung, *Angew. Chem., Int. Ed. Engl.*, 1987, **26**, 1150–1152.
32 M. Kubasik and A. Blom, *ChemBioChem*, 2005, **6**, 1187–1190.
33 R. A. Brown, T. Marcelli, M. De Poli, J. Solà and J. Clayden, *Angew. Chem., Int. Ed.*, 2012, **51**, 1395–1399.
34 B. A. F. Le Bailly, L. Byrne, V. Diemer, M. Foroozandeh, G. A. Morris and J. Clayden, *Chem. Sci.*, 2015, **6**, 2313–2322.
35 B. A. F. Le Bailly, L. Byrne and J. Clayden, *Angew. Chem., Int. Ed.*, 2016, **55**, 2132–2136.
36 J. Brioche, S. J. Pike, S. Tshepelevitsh, I. Leito, G. A. Morris, S. J. Webb and J. Clayden, *J. Am. Chem. Soc.*, 2015, **137**, 6680–6691.
37 F. G. A. Lister, B. A. F. Le Bailly, S. J. Webb and J. Clayden, *Nat. Chem.*, 2017, **9**, 420–425.
38 L. Byrne, J. Solà, T. Boddaert, T. Marcelli, R. W. Adams, G. A. Morris and J. Clayden, *Angew. Chem., Int. Ed.*, 2014, **53**, 151–155.
39 M. Tomsett, I. Maffucci, B. A. F. Le Bailly, L. Byrne, S. M. Bijvoets, M. G. Lizio, J. Raftery, C. P. Butts, S. J. Webb, A. Contini and J. Clayden, *Chem. Sci.*, 2017, **8**, 3007–3018.
40 S. J. Pike, J. E. Jones, J. Raftery, J. Clayden and S. J. Webb, *Org. Biomol. Chem.*, 2015, **13**, 9580–9584.
41 M. De Poli, W. Zawodny, O. Quinonero, M. Lorch, S. J. Webb and J. Clayden, *Science*, 2016, **352**, 575–580.
42 J. Freudenberg and W. H. Binder, *ACS Macro Lett.*, 2020, 686–692, DOI: 10.1021/acsmacrolett.0c00218.
43 H. Kanazawa, *Mol. Cryst. Liq. Cryst. Sci. Technol., Sect. A*, 2006, **313**, 205–210.
44 H. Kanazawa, A. Inada and N. Kawana, *Macromol. Symp.*, 2006, **242**, 104–112.
45 H. Kanazawa and T. Kawai, *J. Polym. Sci., Polym. Chem. Ed.*, 1980, **18**, 629–642.
46 H. Kanazawa and Y. Ohashi, *Mol. Cryst. Liq. Cryst. Sci. Technol., Sect. A*, 1996, **277**, 45–54.
47 H. Kanazawa, Y. Ohashi, Y. Sasada and T. Kawai, *J. Polym. Sci., Polym. Phys. Ed.*, 1982, **20**, 1847–1862.

48 J. Cao, D. Siefker, B. A. Chan, T. Yu, L. Lu, M. A. Saputra, F. R. Fronczek, W. Xie and D. Zhang, *ACS Macro Lett.*, 2017, **6**, 836–840.
49 G. J. M. Habraken, M. Peeters, C. H. J. T. Diezt, C. E. Koning and A. Heise, *Polym. Chem.*, 2010, **1**, 514–524.
50 G. J. M. Habraken, K. H. R. M. Wilsen, C. E. Koning and A. Heise, *Polym. Chem.*, 2011, **2**, 1322–1330.
51 W. Zhao, Y. Gnanou and N. Hadjichristidis, *Polym. Chem.*, 2015, **6**, 6193–6201.
52 Y. Zhang and J. Deng, *Polym. Chem.*, 2020, **11**, 5407–5423.
53 E. Yashima, K. Maeda, H. Iida, Y. Furusho and K. Nagai, *Chem. Rev.*, 2009, **109**, 6102–6211.
54 R. A. G. D. Silva, S. C. Yasui, J. Kubelka, F. Formaggio, M. Crisma, C. Toniolo and T. A. Keiderling, *Biopolymers*, 2002, **65**, 229–243.
55 M. L. Smythe, S. E. Huston and G. R. Marshall, *J. Am. Chem. Soc.*, 1995, **117**, 5445–5452.
56 L. Zhang and J. Hermans, *J. Am. Chem. Soc.*, 1994, **116**, 11915–11921.
57 A. Escobedo, B. Topal, M. B. A. Kunze, J. Aranda, G. Chiesa, D. Mungianu, G. Bernardo-Seisdedos, B. Eftekharzadeh, M. Gairí, R. Pierattelli, I. C. Felli, T. Diercks, O. Millet, J. García, M. Orozco, R. Crehuet, K. Lindorff-Larsen and X. Salvatella, *Nat. Commun.*, 2019, **10**, 2034.
58 R. B. Nellas, Q. R. Johnson and T. Shen, *Biochemistry*, 2013, **52**, 7137–7144.
59 A. Rodger, in *Encyclopedia of Biophysics*, ed. G. C. K. Roberts, Springer Berlin Heidelberg, Berlin, Heidelberg, 2013, pp. 726–730, DOI: 10.1007/978-3-642-16712-6_634.
60 A. Micsonai, F. Wien, L. Kernya, Y.-H. Lee, Y. Goto, M. Réfrégiers and J. Kardos, *Proc. Natl. Acad. Sci. U. S. A.*, 2015, **112**, E3095.
61 G. Nagy, M. Igaev, N. C. Jones, S. V. Hoffmann and H. Grubmüller, *J. Chem. Theory Comput.*, 2019, **15**, 5087–5102.
62 K. Bauri, A. Narayanan, U. Haldar and P. De, *Polym. Chem.*, 2015, **6**, 6152–6162.
63 M. Venanzi, E. Gatto, F. Formaggio and C. Toniolo, *J. Pept. Sci.*, 2017, **23**, 104–116.
64 F. Xu, I. J. Khan, K. McGuinness, A. S. Parmar, T. Silva, N. S. Murthy and V. Nanda, *J. Am. Chem. Soc.*, 2013, **135**, 18762–18765.
65 D. A. Siriwardane, O. Kulikov, Y. Rokhlenko, S. Perananthan and B. M. Novak, *Macromolecules*, 2017, **50**, 9162–9172.
66 E. Yashima, N. Ousaka, D. Taura, K. Shimomura, T. Ikai and K. Maeda, *Chem. Rev.*, 2016, **116**, 13752–13990.
67 B. Czarnik-Matusewicz, S. Pilorz, L.-P. Zhang and Y. Wu, *J. Mol. Struct.*, 2008, **883–884**, 195–202.
68 S. J. Pike, V. Diemer, J. Raftery, S. J. Webb and J. Clayden, *Chem. – Eur. J.*, 2014, **20**, 15981–15990.